3192 *J. Chem. Eng. Data* **2009,** *54,* 3192–3201

Thermodynamic Properties of Propane. II. Molar Heat Capacity at Constant Volume from (85 to 345) K with Pressures to 35 MPa

Richard A. Perkins,* Jesus C. Sanchez Ochoa,† and Joseph W. Magee

Thermophysical Properties Division, Chemical Science and Technology Laboratory, National Institute of Standards and Technology, Boulder, Colorado 80305-3337

Molar heat capacities at constant volume (C_V) were measured with an adiabatic calorimeter for pure propane. The high purity of the samples was verified by chemical analysis. Temperatures ranged from the triple point of propane near 85 K to the upper temperature limit of the calorimeter at 345 K, while pressures ranged up to 35 MPa. Measurements were conducted on liquid propane in equilibrium with its vapor and on compressed liquid samples along isochores. Heat capacity results are reported for two-phase ($C_V^{(2)}$), saturated liquid (C_σ), and single-phase (C_V) isochores. Vapor pressure data are based on measurements of $C_V^{(2)}$ along a two-phase isochore. Measurements were also made to determine the triple-point temperature of (85.525 ± 0.005) K and heat of fusion of (3508 ± 20) J·mol^{-1} for propane near its triple point. The principal sources of uncertainty in C_V are the temperature-rise measurement and the change-of-volume work adjustment. The expanded uncertainty (i.e., a coverage factor $k = 2$ and thus a two-standard deviation estimate) for values of $C_V^{(2)}$ is estimated to be 0.5 %; for both C_σ and C_V, it is 0.7 %.

Introduction

Propane is a common hydrocarbon fuel and is a key component of liquefied petroleum gas (LPG) and natural gas mixtures; it has also been proposed as a component in mixtures for refrigeration cycles. The wide range of reduced temperatures ($T_r = T/T_c$) where propane vapor coexists with liquid, between the triple point T_{tr} and critical point T_c, makes propane an ideal reference fluid for corresponding-states models. This paper is part of a larger effort at NIST[1−3] to develop a reference-quality formulation for the thermophysical properties of propane based on new measurements of density and caloric properties. The isochoric heat capacity of a fluid may be calculated from knowledge of its ideal-gas properties and an equation of state that represents the relationship between temperature (T), pressure (P), and density (ρ). The isochoric heat capacity is given by

$$C_V - C_V^0 = -T\int_0^\rho \left(\frac{\partial^2 P}{\partial T^2}\right)_\rho \frac{d\rho}{\rho^2} \tag{1}$$

where C_V^0 is the ideal-gas heat capacity. The isochoric derivative $(\partial^2 P/\partial T^2)_\rho$ is known to possess small absolute values, except in the vicinity of the critical point, and is difficult to measure directly. Equation 1 provides a means to check for consistency between independent measurements of density and heat capacity, usually through an equation of state.

Molar heat capacities were measured with an adiabatic calorimeter along isochores for single-phase compressed liquid and saturated liquid propane. These measurements cover temperatures from the triple point to 345 K, with compressed liquid isochores at pressures up to 35 MPa. The triple-point temperature, enthalpy of fusion, and vapor pressures are reported, based on evaluation of two-phase heat capacity measurements at temperatures from below the triple point to 345 K.

Experimental Section

Materials. The propane sample used in this work and for density measurements at NIST[1] was specified by the supplier as 99.999 % pure. Our own analysis by gas chromatography combined with mass spectrometry (MS) and infrared spectrophotometry revealed no significant impurities on the total ion chromatogram (MS detection) or total response chromatogram (IR detection). Very small impurity peaks found on the total ion chromatogram were too small to permit identification. Our analysis is consistent with the supplier's purity specification. Measurements of the triple-point temperature described here on this propane sample confirm that this propane sample is quite pure.

Measurements. The adiabatic calorimeter that was used for these measurements was originally described by Goodwin[4] to study hydrogen heat capacity and was used to measure the heat capacity of light hydrocarbons including methane,[5] ethane,[6] (methane + ethane) mixtures,[7] and propane.[8] The calorimeter was improved significantly by Magee[9] prior to measurements on butane.[10] The improvements to the calorimeter by Magee[9] and the high purity of the present sample (99.999 % verified relative to 99.99 % unverified with trace ethane[8]) allow the heat capacity of propane to be measured with lower uncertainty than the earlier results of Goodwin.[8] In addition, the two-phase heat capacity data are used to generate vapor pressure data down to the triple-point temperature, and the triple-point temperature and the associated heat of fusion are reported here.

Details of the calorimeter cell are described in detail by Goodwin[4] and Magee.[9] The present automated data-acquisition and control systems are discussed in detail by Magee.[9] The calorimeter consists of a nearly adiabatic cell that is spherical and has been operated at temperatures from (14 to 345) K with sample pressures up to 35 MPa. Temperatures are measured with a platinum resistance thermometer (SPRT), while pressures are determined with a pressure transducer. During a measurement, a sample of well-established mass is confined within the

---

* Corresponding author. E-mail: richard.perkins@nist.gov.

† Present Address: Instituto Politecnico Nacional, ESIQIE, Zacatenco 07738, Lindavista, Mexico D.F., Mexico.

10.1021/je900137r CCC: $40.75

cell with a well-known volume (approximately 77 cm^3); as shown by Magee,[9] the exact volume varies with both temperature and pressure. After each precisely measured electrical energy (Q) pulse is applied and the cell temperature equilibrates, the resulting temperature rise ($\Delta T = T_2 - T_1$) is measured. The molar heat capacity at constant volume (C_V) of the sample is found by subtracting the energy required to heat the empty bomb (Q_0) and the pressure−volume work (W_{PV}) as

$$C_V = \left(\frac{\partial U}{\partial T}\right)_V \cong \frac{Q - Q_0 - W_{PV}}{n\Delta T} \qquad (2)$$

where n is the amount (mol) of substance.

The sample gas was condensed into the cold sample cell until the cell temperature and pressure indicated that the desired maximum sample density was present in the cell; the charge valve was then closed. The cell and its contents were then cooled to the starting temperature. Each series of heating cycles was started and continued until the upper temperature limit of 345 K was reached or until the maximum pressure of 35 MPa was reached for single-phase samples. At the completion of a pseudoisochore, some of the sample was discharged into a weighing cylinder to obtain the next filling density. A series of difference weighings of a sample collection cylinder gave the sample mass for each isochore after the remaining sample from the final isochore was collected. A series of such isochores at different densities (ρ) completed the $C_V(\rho,T)$ surface for the sample.

The energy required to heat the empty cell (Q_0) from the initial temperature (T_1) to the final temperature (T_2) was found from previous experiments with the cell thoroughly evacuated.[9] The model that represents these empty cell results is described by Magee[9] and is the basis for evaluation of Q_0 in the analysis of the present measurements with eq 2. The pressure−volume work (W_{PV}) accounts for the work done by the fluid on the thin-walled bomb as the pressure rises from P_1 to P_2. Calculation of the pressure−volume work is discussed by Goodwin and Weber[11] and is given by

$$W_{PV} = \left(T_2\left(\frac{\partial P}{\partial T}\right)_{V_2} - \frac{\Delta P}{2}\right)\Delta V \qquad (3)$$

where $\Delta P = P_2 - P_1$ is the pressure rise and $\Delta V = V_2 - V_1$ is the volume increase. The pressure derivative has been calculated with the equation of state of Lemmon et al.[3] for propane.

The amount (mol) of substance n contained in the cell varies slightly due to the noxious volume that is about 0.2 % of the cell volume.[9] This noxious volume is the sum of the volumes of the pressure transducer, charging valve, and capillary tubing. The valve and pressure transducer are contained in an isothermal aluminum block that is controlled at a temperature near 320 K such that the temperature gradient occurs along a small capillary tube between the cell and this isothermal assembly. The amount of the sample in this noxious volume is obtained from the measured volumes and the density calculated with the equation of state[3] at the measured pressure and temperature of the pressure transducer/valve assembly and assuming a quadratic temperature profile along the length of the capillary. The molar mass for propane of 44.096 g·mol^{-1}, based on the atomic weights of the elements,[12] was used throughout this work.

Results

Triple-Point Temperature. Measurements of the triple point of propane provide a check of the purity of the sample since an impure sample will exhibit freezing-point depression. The triple-point temperature of propane has been extensively studied by Pavese and Besley[13] who report a value of (85.528 ± 0.003) K converted from the IPTS-68 temperature scale to ITS-90.[14] Pavese and Besley[13] observed a depression in the freezing point of 6 mK that indicated impurities of the order of 0.0001 mol fraction in their propane sample. Hicks-Brunn and Brunn[15] reported 86.016 K, while Kemp and Egan[16] reported 85.465 K, for the triple point temperature of propane (ITS-90). Given the level of uncertainty available in 1995, the value of 85.53 K was recommended[17] for the triple-point temperature of propane.

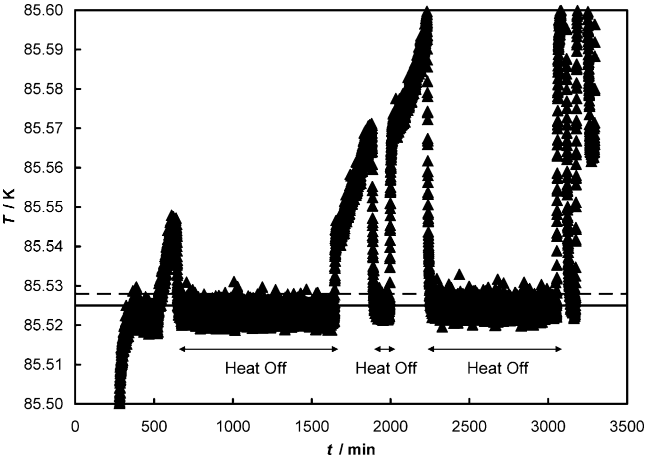

Figure 1. Measured calorimeter temperature as propane is melted near its triple point. Filled triangles are measured temperatures, while the solid line is our triple-point temperature at 85.525 K. The dashed line at 85.528 K is the value reported by Pavese and Besley[13] for the triple-point temperature.

The present propane sample is 99.999 % pure relative to the 99.99 % pure sample studied by Pavese and Besley;[13] the freezing point depression should be less. Pavese and Besley[13] reported temperatures that vary from 28 mK low at 0.2 melt fraction to 6 mK low at 0.9 melt fraction. Subcooling of (3 to 8) K below the triple point was required to freeze the propane sample in the calorimeter. Figure 1 shows the measured temperature as a function of time that we observed for propane near its triple point. The average temperature was measured at various melt fractions without heating, as indicated by the nearly isothermal regions between the heating stages. The elapsed time for each period without cell heating was arbitrary and up to 16 h, demonstrating that melting was very slow due to the adiabatic characteristics of the calorimeter. At 0.1 melt fraction, we observed a temperature that was only about 3 mK lower than that measured at 0.9 melt fraction. Thus, there was very little depression in the freezing point for the present sample of propane. The triple-point temperature averaged over each unheated period for the melt fractions of 0.5 and 0.9 was 85.525 K, with a standard deviation of 0.0017 K. Freezing point depression was less than 1 mK for this high-purity sample and, a selection of melt fractions greater that 0.5 for averaging reduces its influence on the measured triple point. The uncertainty in the present measurement of the triple-point temperature of propane was less than 0.005 K. There was little contribution to this uncertainty due to purity of the sample (freezing-point depression). The largest contribution to the uncertainty is due to temperature gradients between the cell and the standard platinum resistance thermometer (SPRT). These temperature gradients should be small (about 0.003 K) when no heat is applied to the calorimeter. Our final value for the triple-point temperature is (85.525 ± 0.005) K. The noise level in the temperature measurement was characterized by the standard deviation of the averaged temperature of 0.0016 K.

The triple point of argon was also measured to verify the measurement procedure and the calibration of the SPRT. The measured argon triple point was 0.003 K higher than the ITS-90 fixed point value of 83.8058 K.[14] The temperature noise was 0.003 K at a coverage factor of $k = 2$ for both propane and the measurement of the triple point of argon that is described in the Supporting Information.

Enthalpy of Fusion. The frozen sample was heated at a constant power of 0.0817 W while the temperature was recorded. The enthalpy of fusion $\Delta_{\mathrm{fus}}H$ was measured by integrating the applied heater power over the period of melting and applying corrections for heating of the calorimeter and parasitic heat losses. The onset of melting was indicated by a plateau in the temperature at fixed heating power. The measured temperature starts out near the triple-point temperature when melting begins but slowly increases as the thickness of the liquid layer increases between the cell wall and the melting solid. The temperature again rises more rapidly when the last of the solid propane has melted. The results and expanded uncertainties ($k = 2$) for $\Delta_{\mathrm{fus}}H$ obtained from two experiments were (3506 ± 20) J·mol^{-1} and (3511 ± 20) J·mol^{-1}; the average of (3508 ± 20) J·mol^{-1} is the best estimate for $\Delta_{\mathrm{fus}}H$ at the triple point from these measurements. These values agree well with those reported by Pavese and Besley[13] of (3500 ± 25) J·mol^{-1} and Kemp and Egan[16] of (3525 ± 4) J·mol^{-1}.

Isochoric Heat Capacity. The values measured for the isochoric heat capacity C_{V} of propane are given in Table 1 at 231 single-phase states. The average of the initial and final temperatures for each heating interval is given for the temperature (ITS-90) of each data point. The tabulated pressures are calculated from a least-squares fit of the (P, T) data using a seven-term function given by

$$P = \frac{c_1}{T_{\mathrm{r}}^4} + \frac{c_2}{T_{\mathrm{r}}^3} + \frac{c_3}{T_{\mathrm{r}}^2} + \frac{c_4}{T_{\mathrm{r}}} + c_5 + c_6\sqrt{T_{\mathrm{r}}} + c_7 T_{\mathrm{r}} \qquad (4)$$

where c_i are the fit coefficients for the isochore, and $T_{\mathrm{r}} = T/T_{\mathrm{c}}$, with T_{c} equal to the critical temperature of propane (369.89 K).[3] The density is calculated from the corrected amount (mol) of sample and the calibrated bomb volume described in the Supporting Information. Since the density of propane is known with very low uncertainty, it is an ideal material for improved calibration of the bomb volume (previously known with a relative uncertainty of 0.15 %). Since the calibration of the bomb volume is based on densities calculated with the equation of state of Lemmon et al.,[3] comparison of the reported densities with this same equation of state has little value in assessing the uncertainty of the density data for propane. Nonetheless, the densities reported in Table 1 are consistent (with a relative uncertainty of 0.012 %) with the equation of state of Lemmon et al.,[3] the filling mass, and the calibrated cell volume that was used for pressure−volume work adjustments.

Values of the single-phase heat capacity of the liquid are shown in Figure 2 at temperatures from (102 to 345) K with pressures up to 35 MPa. The data are measured along isochores with increasing temperature and pressure. Most of the isochores overlap in their temperature ranges, except at the highest densities, where C_{V} is observed to increase. Figure 3 shows deviations between these measured C_{V} data and literature data,[8,18] relative to values calculated with the equation of state of Lemmon et al.[3] Agreement is within 1.45 % ($k = 2$ standard deviation uncertainty) over the entire temperature region from (100 to 340) K. The C_{V} data are 1 % to 2 % higher than the equation-of-state calculations of Lemmon et al.[3] over the temperature region from (180 to 260) K. Scatter in the C_{V} data, due primarily to thermally induced noise, increases with temperature but remains within the estimated uncertainty of 0.7 %. Good agreement (± 1 %) is found with the previous measurements of Goodwin[8] and the measurements of Anisimov et al.[18] At the lowest temperatures, the data of Goodwin[8] are systematically higher than both the present results and the equation of state of Lemmon et al.[3] At these low reduced temperatures, the propane is very incompressible, and the compression work correction is large and extremely sensitive to errors in volume change of the calorimeter cell. The excellent agreement between the present measurements at temperatures near 100 K and the equation of state provides confirmation that the cell volume calibration described in the Supporting Information is accurate. The liquid data of Abdulagatov et al.[19] are systematically 2 % to 8 % higher than the other data for compressed liquid states relative to the equation of state of Lemmon et al.[3] over this temperature range and are not shown in Figure 3.

Heat Capacity of the Saturated Liquid. The values measured for the saturated liquid heat capacity C_σ of propane are given in Table 2 at 223 two-phase states. The average of the initial and final temperatures for each heating interval is given for the temperature (ITS-90) of each data point. Most of the measured vapor pressures are below the most accurate range of the pressure gauge [(3 to 70) MPa]. Thus, the vapor pressure and the density of the saturated liquid were calculated with the equation of state[3] at the average temperature of the heating interval. Values of the two-phase heat capacity at constant volume ($C_{\mathrm{V}}^{(2)}$) are presented as well as values of the saturated-liquid liquid heat capacity C_σ. Values of C_σ are obtained by adjusting the $C_{\mathrm{V}}^{(2)}$ data with the equation given by Rowlinson[20]

$$C_\sigma = C_{\mathrm{V}}^{(2)} - \frac{T}{\rho_\sigma^{\,2}}\left(\frac{d\rho_\sigma}{dT}\right)\left(\frac{dP_\sigma}{dT}\right) + T\left(\frac{1}{\rho_\sigma} - \frac{1}{\rho}\right)\frac{d^2P_\sigma}{dT^2} \qquad (5)$$

where P_σ and ρ_σ are the pressure and density of the saturated liquid and ρ is the bulk density of the sample residing in the bomb. The derivative quantities were all calculated with the equation of state of Lemmon et al.[3]

The saturated-liquid heat capacity C_σ depends only on the temperature. If the data are internally consistent, then the values at saturation measured at different filling densities should fall on a single curve. The present C_σ values were evaluated from experiments with two different amounts of sample in the calorimeter, and the results for two isochors with differing amounts of sample [(0.89 and 0.61) mol] are consistent with each other, as shown in Figures 4 and 5. Figure 4 shows the present data for C_σ at temperatures from (89 to 344) K, along with the previous data of Goodwin[8] and values calculated with the equation of state of Lemmon et al.[3] Figure 5 shows deviations between the data for C_σ at temperatures from (88 to 356) K and the values calculated with the equation of state. The present results are up to 0.5 % higher than the previous data of Goodwin[8] and extend the upper temperature limit of the available data for C_σ from (300 to 345) K. Agreement between the two data sets is good and within the estimated uncertainty of 0.7 % for the present measurements. Low-temperature C_{P} (< 0.1 MPa) data that are nearly equal to C_σ are also compared with the present measurements in Figure 5. The C_{P} data of Cutler and Morrison[21] are 0.5 % to 1.5 % lower than the present C_σ data, while the C_{P} data of Kemp and Egan[16] agree with the present C_σ data to within 0.5 %. Values calculated with the equation of state of Lemmon et al.[3] agree with the

Table 1. Values Measured for the Isochoric Heat Capacity C_V of Propane at Temperatures from (102 to 345) K with Pressures up to 35 MPa

T	ρ	P	C_V	T	ρ	P	C_V	T	ρ	P	C_V
K	$(\text{mol}\cdot\text{L}^{-1})$	MPa	$(\text{J}\cdot\text{mol}^{-1}\cdot\text{K}^{-1})$	K	$(\text{mol}\cdot\text{L}^{-1})$	MPa	$(\text{J}\cdot\text{mol}^{-1}\cdot\text{K}^{-1})$	K	$(\text{mol}\cdot\text{L}^{-1})$	MPa	$(\text{J}\cdot\text{mol}^{-1}\cdot\text{K}^{-1})$
102.314	16.307	9.415	59.63	235.918	13.382	13.904	65.71	287.263	12.004	10.490	72.25
105.245	16.291	15.961	59.93	238.456	13.376	16.299	66.07	289.949	11.999	12.212	72.29
108.151	16.276	22.430	60.17	240.986	13.370	18.681	66.68	292.636	11.995	13.928	73.17
111.017	16.261	28.556	60.44	243.503	13.364	21.054	66.99	295.336	11.990	15.644	73.82
101.140	16.317	5.078	59.59	246.014	13.359	23.413	67.65	298.045	11.986	17.358	74.20
104.092	16.297	13.618	59.63	248.525	13.353	25.750	67.69	300.759	11.982	19.068	74.45
107.010	16.283	19.580	59.80	251.020	13.347	28.035	68.22	303.478	11.977	20.773	74.78
109.893	16.267	26.296	60.20	253.516	13.342	30.287	68.63	306.203	11.973	22.473	75.56
126.589	15.751	8.062	59.47	256.003	13.337	32.529	69.58	308.939	11.969	24.172	76.12
129.392	15.738	13.480	59.66	224.720	13.408	3.002	64.29	311.684	11.964	25.869	76.11
132.167	15.726	18.723	60.02	227.279	13.402	5.514	64.59	314.428	11.960	27.556	77.06
134.918	15.714	23.869	60.12	229.837	13.396	8.010	64.80	317.183	11.956	29.242	77.79
137.642	15.702	28.865	60.52	232.385	13.390	10.480	64.79	319.955	11.951	30.930	77.48
124.992	15.759	4.945	59.16	234.924	13.384	12.923	65.31	322.733	11.947	32.614	78.00
127.809	15.746	10.414	59.44	237.464	13.378	15.350	65.71	301.578	11.209	3.377	74.41
130.597	15.733	15.739	59.60	239.990	13.372	17.746	65.96	304.371	11.206	4.801	74.97
133.360	15.721	20.943	60.00	242.515	13.367	20.123	66.43	307.189	11.202	6.235	74.97
136.097	15.708	26.024	60.14	245.026	13.361	22.471	67.42	310.014	11.198	7.669	75.56
138.812	15.697	30.978	60.43	247.539	13.355	24.804	67.75	312.848	11.194	9.104	76.02
150.881	15.193	6.488	59.62	250.037	13.350	27.105	67.70	315.695	11.190	10.543	77.05
153.586	15.182	10.968	60.10	252.529	13.344	29.385	68.06	318.555	11.187	11.984	77.31
156.271	15.172	15.303	60.05	255.019	13.339	31.645	68.71	321.426	11.183	13.428	77.25
158.933	15.162	19.535	60.50	250.677	12.749	3.498	66.65	324.312	11.179	14.874	77.39
161.582	15.152	23.733	60.93	253.263	12.743	5.557	67.47	327.218	11.175	16.325	78.34
164.206	15.142	27.828	61.20	255.851	12.738	7.667	67.82	330.147	11.171	17.784	78.59
166.812	15.133	31.798	61.54	258.438	12.733	9.764	67.88	333.090	11.167	19.244	78.85
149.778	15.197	4.666	59.78	261.016	12.728	11.824	68.53	336.053	11.163	20.709	79.20
152.481	15.186	9.113	59.99	263.601	12.723	13.861	69.03	339.048	11.159	22.184	80.79
155.170	15.176	13.482	60.14	266.184	12.718	15.878	69.32	342.070	11.155	23.667	81.31
157.840	15.166	17.768	60.44	268.759	12.713	17.881	69.68	300.727	11.211	2.939	74.37
160.488	15.156	21.973	60.63	271.334	12.708	19.881	70.43	303.535	11.207	4.354	74.77
163.118	15.146	26.095	60.76	273.905	12.703	21.877	70.90	306.356	11.203	5.801	74.54
165.731	15.136	30.131	61.05	276.476	12.698	23.865	71.62	309.185	11.199	7.252	75.53
175.512	14.621	5.348	60.54	279.043	12.693	25.835	72.09	312.044	11.195	8.706	75.83
178.150	14.612	9.061	60.86	281.614	12.689	27.786	72.29	314.907	11.191	10.151	75.71
180.774	14.604	12.700	61.22	284.186	12.684	29.713	72.65	317.790	11.188	11.598	77.05
183.379	14.595	16.221	61.34	286.768	12.679	31.632	72.64	320.706	11.184	13.058	77.40
185.968	14.587	19.691	61.79	289.342	12.674	33.552	73.33	323.623	11.180	14.518	78.11
188.543	14.579	23.141	62.12	249.660	12.751	2.670	66.76	326.571	11.176	15.995	78.02
191.100	14.571	26.538	62.39	252.252	12.745	4.769	67.25	329.524	11.172	17.472	78.67
193.642	14.563	29.843	62.88	254.848	12.740	6.861	67.69	332.503	11.168	18.957	79.25
196.165	14.555	33.063	63.39	257.440	12.735	8.938	67.87	335.497	11.164	20.439	79.93
174.725	14.624	4.244	60.48	260.025	12.730	10.999	68.40	338.525	11.160	21.926	80.26
177.359	14.615	7.916	60.58	262.613	12.725	13.051	68.83	341.560	11.156	23.408	80.54
179.972	14.606	11.523	61.04	265.199	12.720	15.091	69.38	344.623	11.152	24.907	81.87
182.573	14.598	15.077	61.29	267.786	12.715	17.120	69.94	301.673	11.209	3.419	74.62
185.156	14.590	18.570	61.57	270.370	12.710	19.134	70.51	304.509	11.206	4.850	74.76
187.722	14.582	22.005	62.06	272.953	12.705	21.136	70.81	307.353	11.202	6.310	75.30
190.273	14.574	25.385	62.49	275.538	12.700	23.127	70.92	310.220	11.198	7.778	75.78
192.807	14.566	28.708	62.66	278.118	12.695	25.101	71.49	313.104	11.194	9.241	76.23
195.331	14.558	31.980	62.87	280.700	12.690	27.065	72.08	315.995	11.190	10.697	76.49
200.293	14.034	4.569	62.02	283.286	12.686	29.020	72.18	318.910	11.186	12.158	77.07
202.878	14.027	7.627	62.29	285.870	12.681	30.962	72.47	321.834	11.182	13.623	76.95
205.454	14.019	10.675	62.72	288.454	12.676	32.894	72.96	324.769	11.178	15.094	77.50
208.017	14.012	13.633	63.07	276.184	12.022	3.327	70.24	327.727	11.174	16.576	78.56
210.568	14.005	16.525	63.38	278.848	12.017	5.025	70.73	330.698	11.170	18.059	79.38
213.107	13.998	19.392	63.48	281.506	12.013	6.761	71.44	333.684	11.167	19.542	80.20
215.631	13.992	22.244	63.92	284.175	12.009	8.508	71.57	336.698	11.163	21.027	80.28
218.145	13.985	25.069	64.71	286.850	12.004	10.247	71.76	339.730	11.159	22.511	80.76
220.656	13.978	27.850	64.89	289.520	12.000	11.964	71.92	342.794	11.155	24.013	81.23
223.143	13.972	30.548	65.25	292.199	11.996	13.671	72.85	321.301	10.393	2.771	77.58
225.628	13.965	33.221	66.00	294.875	11.991	15.364	73.57	324.353	10.389	3.977	78.06
199.291	14.037	3.434	62.08	297.559	11.987	17.055	74.47	327.420	10.386	5.191	78.96
201.885	14.029	6.487	62.05	300.256	11.983	18.750	74.37	330.514	10.382	6.416	78.78
204.464	14.022	9.498	62.44	302.951	11.978	20.442	74.16	333.625	10.379	7.647	78.71
207.029	14.015	12.468	63.03	305.646	11.974	22.131	75.52	336.760	10.375	8.887	79.06
209.590	14.008	15.407	63.29	308.366	11.970	23.829	76.01	339.915	10.372	10.135	80.44
212.128	14.001	18.295	63.46	311.085	11.965	25.517	76.58	343.098	10.368	11.393	80.84
214.660	13.994	21.152	63.90	313.822	11.961	27.203	77.38	319.667	10.394	2.142	76.76
217.181	13.988	23.972	64.21	316.578	11.957	28.887	76.95	322.713	10.391	3.326	77.29
219.686	13.981	26.749	64.74	319.328	11.952	30.553	77.02	325.781	10.388	4.543	78.25
222.182	13.974	29.491	65.36	322.103	11.948	32.227	78.59	328.878	10.384	5.770	78.35
224.672	13.968	32.203	65.68	324.906	11.944	33.925	78.84	331.988	10.381	6.999	78.63
225.690	13.406	3.945	64.40	276.561	12.021	3.559	70.86	335.123	10.377	8.240	79.20
228.261	13.400	6.458	64.54	279.230	12.017	5.297	71.29	338.277	10.374	9.489	80.76
230.819	13.394	8.990	65.20	281.903	12.012	7.032	70.95	341.461	10.370	10.747	81.71
233.375	13.388	11.478	65.49	284.576	12.008	8.760	71.75	344.670	10.367	12.011	81.35

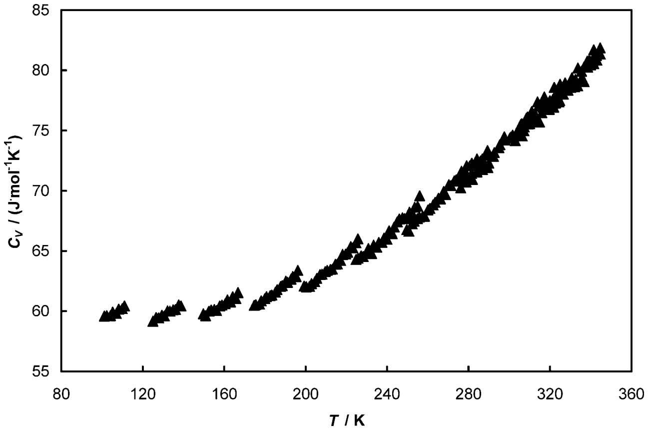

Figure 2. Measured isochoric heat capacity (C_V) of propane at temperatures from (102 to 345) K with pressures up to 35 MPa.

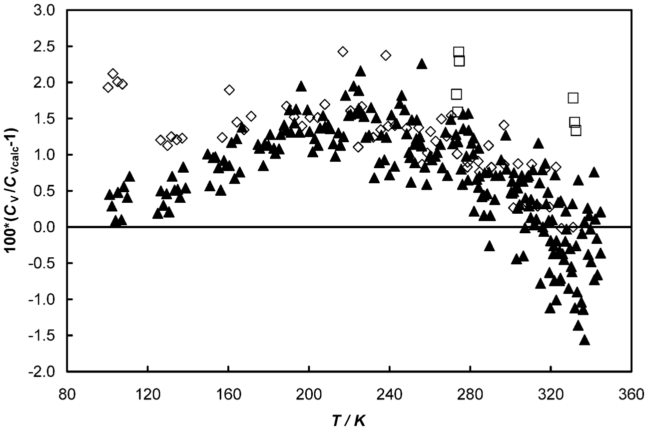

Figure 3. Relative deviations between measured isochoric heat capacity (C_V) of propane and values calculated with the equation of state of Lemmon et al.[3] at temperatures from (102 to 345) K with pressures up to 35 MPa, where: ▲, present results; ◇, Goodwin;[8] and □, Anisimov et al. [18]

experimental data to within 0.9 % ($k = 2$ standard deviation uncertainty) from the triple-point temperature to 345 K. The present data are up to 2 % lower than the values with the equation of state of Lemmon et al.[3] at their maximum temperature near 345 K. The maximum deviation in C_σ relative to Lemmon et al.[3] coincides with the maximum difference between the measured $C_V^{(2)}$ data and the C_σ values obtained from eq 5 and given in Table 2. Equation 5 is increasingly sensitive to uncertainties in the first and second derivatives of the vapor-pressure curve as the temperature increases, although the difference between the sample density and the saturated liquid density decreases in the right-most term.

Derived Vapor Pressure. Accurate measurement of the vapor pressure of a liquid becomes increasingly difficult at temperatures below the normal boiling point. Glos et al.[22] report the normal boiling point temperature of propane to be 231.036 K. Very dilute, but volatile, impurities in a sample can introduce errors in direct measurements of vapor pressure that are difficult to quantify when the partial pressure of an impurity becomes significant relative to the partial pressure of the sample. Dynamic techniques such as ebulliometry, effusion, and gas saturation that purge volatile impurities from the gas phase are effective at reducing such errors. It remains difficult to measure pressure accurately for samples that are at less than ambient pressure since most pressure sensors actually measure pressure differences relative to high vacuum, and the absolute value of the pressure difference can be extremely small. Vapor-pressure data have been reported at temperatures below 240 K by four groups. The recent work of Glos et al.[22] covered the temperature range from (110 to 340) K with very accurate direct measurement of the vapor pressure. Tickner and Lossing[23] covered the temperature range from (105 to 165) K with vapor pressures determined from propane flow through a calibrated orifice, quantified by the ion peak intensity from a mass spectrometer. Carruth and Kobayashi[24] covered the temperature range from (95 to 179) K with vapor pressures obtained from a gas-saturation technique. Finally, Kemp and Egan[16] covered the temperature range from (166 to 232) K by direct measurement of the vapor pressure with a mercury manometer.

Duarte-Garza and Magee[25] have shown that vapor-pressure values can be derived from measurements of the two-phase heat capacity $C_V^{(2)}$ that are described above. The $C_V^{(2)}$ values described above have an excellent internal consistency and have their lowest uncertainty below the normal boiling point because the necessary adjustments to the $C_V^{(2)}$ measurements for vaporization and pV work are less than 0.1 % of the resulting $C_V^{(2)}$ value. Vapor pressure values derived from these $C_V^{(2)}$ data should have a low uncertainty from the triple point at 85.525 K up to the vicinity of the normal boiling point at 231.036 K.

In the present work, only a brief summary is given for the technique to derive vapor pressures from isochoric internal-energy measurements in the two-phase region. A detailed discussion is presented by Duarte-Garza and Magee.[25] The method is based on the expression relating the two-phase internal energy $U^{(2)}(T, V)$ to the vapor pressure

$$\left(\frac{\partial U^{(2)}}{\partial V^{(2)}}\right)_T = T\left(\frac{dP_\sigma}{dT}\right) - P_\sigma = T^2\left(\frac{d(P_\sigma/T)}{dT}\right) \qquad (6)$$

where the subscript σ signifies a quantity evaluated along the liquid−vapor saturation boundary. Because of the linear dependence of $U^{(2)}$ on the molar volume V, the derivative on the left side of eq 6 can be replaced exactly with a finite-difference expression

$$\left(\frac{\partial U^{(2)}}{\partial V^{(2)}}\right)_T = \left(\frac{U_2^{(2)} - U_1^{(2)}}{V_2^{(2)} - V_1^{(2)}}\right)_T \qquad (7)$$

where subscripts 1 and 2 indicate any two state points within the two-phase region, including the single-phase liquid or vapor at saturation, and the superscript (2) indicates the bulk property. In this work, a bulk property is any property of the vapor in equilibrium with the liquid combined in proportion to their molar phase ratios.

After computing $(\partial U^{(2)}/\partial V^{(2)})_T$ at different temperatures between the triple point and the normal boiling point with eq 7, we can fit eq 6 to these data using a nonlinear regression analysis of the parameters in an equation for $P_\sigma(T)$. As indicated by eq 6, the regression analysis must fit the adjustable parameters in the difference expression $T(dP_\sigma/dT) - P_\sigma$. Once an expression for $P_\sigma(T)$ is selected that can accurately represent the vapor pressure over a wide range of temperature, its analytic derivative (dP_σ/dT) is determined so that the difference expression $T(dP_\sigma/dT) - P_\sigma$ depends only on T and the parameters in the equation for $P_\sigma(T)$. In principle, nonlinear regression could be used to simultaneously fit a vapor pressure equation to P_σ data and to $U^{(2)}$ data, but only the $U^{(2)}(T, V)$ data are fit in the present work because these data are very weakly affected by volatile impurities and they extend down to temperatures near the triple point.

Experimental values for $U^{(2)}$ at precisely known densities are required to carry out the calculations with eq 7. We use the energy-increment data from the present isochoric (constant $V^{(2)}$)

Table 2. Values Measured for the Two-Phase Isochoric Heat Capacity $C_V^{(2)}$ and the Saturated Liquid Heat Capacity C_σ of Propane at Temperatures from (88 to 345) K

T	ρ_σ	P_σ	$C_V^{(2)}$	C_σ	T	ρ_σ	P_σ	$C_V^{(2)}$	C_σ	T	ρ_σ	P_σ	$C_V^{(2)}$	C_σ
K	(mol·L^{-1})	Pa	(J·mol^{-1}·K^{-1})	(J·mol^{-1}·K^{-1})	K	(mol·L^{-1})	Pa	(J·mol^{-1}·K^{-1})	(J·mol^{-1}·K^{-1})	K	(mol·L^{-1})	Pa	(J·mol^{-1}·K^{-1})	(J·mol^{-1}·K^{-1})
							$n = 0.69081$ mol							
88.919	16.546	0.00064938	84.87	84.87	267.899	12.146	402810.	109.49	107.71	185.912	14.297	7902.1	92.28	92.02
92.731	16.456	0.0025475	84.92	84.92	267.923	12.146	403120.	109.35	107.58	188.683	14.230	9625.2	92.38	92.09
96.466	16.369	0.0086807	84.96	84.96	270.423	12.071	436160.	110.19	108.40	191.440	14.164	11636.	93.05	92.72
100.130	16.283	0.026244	85.19	85.19	272.919	11.995	471120.	110.94	109.16	194.184	14.098	13970.	93.42	93.05
103.730	16.200	0.071643	85.36	85.36	275.416	11.918	508140.	111.85	110.08	196.908	14.032	16652.	93.97	93.56
107.273	16.118	0.17916	85.47	85.47	277.917	11.840	547350.	112.19	110.44	199.622	13.966	19729.	94.48	94.02
110.757	16.037	0.41451	85.79	85.79	280.408	11.761	588590.	113.16	111.44	202.325	13.900	23238.	94.58	94.07
114.194	15.958	0.89751	85.97	85.97	282.911	11.681	632310.	113.74	112.06	205.010	13.834	27208.	94.92	94.36
117.582	15.880	1.8309	86.14	86.14	285.409	11.600	678280.	113.88	112.26	207.688	13.767	31696.	95.53	94.92
120.931	15.803	3.5475	86.45	86.45	287.910	11.517	726730.	114.66	113.12	210.350	13.701	36729.	96.07	95.41
124.234	15.727	6.5535	86.54	86.53	290.414	11.433	777750.	116.21	114.75	213.004	13.635	42364.	96.78	96.05
127.503	15.653	11.621	86.90	86.90	292.929	11.348	831600.	116.86	115.51	215.646	13.569	48640.	97.16	96.38
130.733	15.579	19.835	87.09	87.09	295.440	11.261	888050.	118.11	116.88	218.276	13.502	55600.	97.98	97.14
133.929	15.505	32.729	87.32	87.31	297.962	11.173	947530.	118.93	117.85	220.904	13.435	63320.	97.84	96.94
137.096	15.433	52.395	87.68	87.67	300.484	11.082	1009900.	118.87	117.96	223.515	13.368	71806.	98.24	97.28
140.231	15.361	81.548	87.61	87.61	303.012	10.990	1075300.	119.09	118.38	226.119	13.301	81135.	99.20	98.17
143.335	15.290	123.70	87.92	87.91	305.539	10.896	1143800.	120.11	119.64	228.724	13.234	91394.	99.74	98.66
146.410	15.219	183.27	88.37	88.35	308.075	10.800	1215700.	121.73	121.52	231.309	13.166	102550.	100.25	99.11
149.460	15.149	265.85	88.46	88.44	310.617	10.702	1291000.	122.38	122.47	233.897	13.098	114750.	100.84	99.63
152.476	15.080	377.76	88.74	88.71	313.154	10.601	1369500.	124.20	124.63	236.472	13.030	127990.	100.90	99.64
155.471	15.010	527.35	89.04	89.00	315.709	10.497	1452100.	125.06	125.89	239.041	12.961	142340.	101.53	100.21
158.447	14.942	724.31	89.30	89.26	318.273	10.391	1538500.	125.12	126.41	241.607	12.892	157880.	102.32	100.94
161.404	14.873	979.83	89.49	89.43	323.352	10.170	1720800.	126.92	129.31	244.167	12.823	174650.	103.24	101.80
164.340	14.805	1306.6	89.60	89.53	325.931	10.054	1819200.	128.22	131.30	246.725	12.753	192750.	104.15	102.66
167.249	14.737	1718.1	90.15	90.06	328.509	9.933	1921700.	129.53	133.40	249.279	12.682	212210.	104.71	103.18
170.141	14.669	2231.9	90.47	90.37	331.101	9.808	2028900.	131.20	135.99	251.826	12.611	233070.	105.21	103.62
173.013	14.602	2865.7	90.41	90.28	333.701	9.678	2140800.	131.83	137.68	254.373	12.539	255460.	105.70	104.07
175.862	14.535	3638.4	91.06	90.91	336.310	9.541	2257700.	131.99	139.10	256.920	12.467	279450.	106.14	104.47
178.697	14.468	4574.4	91.35	91.17	338.929	9.399	2379800.	132.37	140.95	259.461	12.394	305040.	106.68	104.97
181.513	14.401	5696.0	91.51	91.30	341.563	9.248	2507400.	134.29	144.64	262.000	12.321	332330.	107.73	106.00
184.309	14.335	7028.1	91.99	91.75	344.209	9.089	2640800.	136.64	149.14	264.542	12.246	361460.	107.86	106.11
187.093	14.268	8602.2	92.50	92.23	91.121	16.494	0.0014520	84.92	84.92	267.076	12.171	392360.	108.94	107.17
189.855	14.202	10442.	92.88	92.57	94.890	16.405	0.0052413	85.02	85.02	269.623	12.095	425370.	109.42	107.64
192.606	14.136	12585.	93.23	92.88	98.583	16.319	0.016631	85.12	85.12	272.154	12.018	460190.	110.81	109.03
195.337	14.070	15058.	94.06	93.67	102.209	16.235	0.047315	85.32	85.32	274.698	11.940	497280.	111.41	109.64
198.058	14.004	17904.	94.38	93.95	105.775	16.152	0.12260	85.44	85.44	277.238	11.861	536490.	111.97	110.22
200.763	13.938	21154.	94.60	94.12	109.282	16.071	0.29270	85.76	85.76	279.779	11.781	577970.	112.55	110.83
203.454	13.872	24846.	95.21	94.68	112.742	15.991	0.65170	85.84	85.84	282.322	11.700	621810.	113.32	111.64
206.138	13.806	29031.	94.80	94.22	116.151	15.913	1.3624	86.05	86.05	284.864	11.617	668040.	114.56	112.93
208.802	13.740	33730.	95.18	94.54	119.513	15.836	2.6944	86.16	86.16	287.407	11.534	716790.	115.51	113.95
211.454	13.674	38995.	96.27	95.58	122.833	15.760	5.0741	86.51	86.51	289.953	11.449	768170.	116.12	114.64
214.102	13.607	44889.	96.99	96.24	126.117	15.684	9.1519	86.66	86.66	292.497	11.363	822160.	116.84	115.46
216.732	13.541	51424.	97.50	96.69	129.363	15.610	15.868	86.88	86.88	295.043	11.275	878940.	117.61	116.36
219.354	13.475	58671.	98.27	97.40	132.570	15.537	26.539	87.08	87.07	297.591	11.186	938600.	118.65	117.55
221.971	13.408	66686.	98.36	97.43	135.749	15.464	43.021	87.22	87.22	300.145	11.095	1001300.	119.87	118.94
224.571	13.341	75481.	98.56	97.58	138.895	15.392	67.722	87.51	87.50	302.694	11.002	1066900.	120.41	119.67
227.162	13.274	85128.	99.44	98.39	142.010	15.320	103.80	87.95	87.94	305.254	10.907	1135900.	120.99	120.48
229.748	13.207	95694.	100.10	98.99	145.104	15.249	155.45	88.07	88.06	307.817	10.810	1208200.	121.27	121.03
232.326	13.139	107220.	100.66	99.49	148.164	15.179	227.47	88.35	88.33	310.381	10.711	1283900.	122.57	122.63
234.899	13.072	119770.	100.63	99.41	151.202	15.109	326.29	88.75	88.72	312.955	10.609	1363300.	123.52	123.93
237.459	13.004	133360.	101.40	100.12	154.211	15.040	459.12	88.86	88.83	315.533	10.504	1446300.	123.95	124.76
240.020	12.935	148120.	101.84	100.50	157.196	14.971	634.91	89.10	89.06	318.115	10.397	1533100.	124.11	125.37
242.568	12.866	164020.	102.60	101.20	160.151	14.902	863.41	89.71	89.66	323.238	10.176	1716600.	126.64	129.01
245.118	12.797	181220.	103.24	101.78	163.085	14.834	1157.0	90.11	90.05	325.837	10.058	1815600.	127.13	130.18
247.660	12.727	199710.	103.78	102.27	166.004	14.766	1530.2	90.12	90.04	328.442	9.936	1919000.	128.49	132.33
250.201	12.656	219590.	104.54	102.98	168.904	14.698	1998.1	90.34	90.24	331.060	9.810	2027200.	130.27	135.04
252.738	12.585	240910.	105.01	103.41	171.786	14.631	2578.5	90.50	90.38	333.691	9.678	2140400.	130.59	136.44
255.269	12.514	263720.	105.64	103.99	174.647	14.564	3289.8	91.03	90.89	336.317	9.541	2258000.	131.93	139.03
257.801	12.442	288130.	106.24	104.55	177.489	14.497	4153.5	91.42	91.25	338.958	9.397	2381100.	134.13	142.73
260.325	12.369	314130.	107.10	105.39	180.314	14.430	5193.2	91.86	91.67	341.609	9.245	2509700.	135.58	145.97
262.854	12.296	341910.	108.10	106.36	183.121	14.363	6433.5	92.07	91.84	344.273	9.085	2644100.	135.80	148.36
265.381	12.221	371480.	108.22	106.45										
							$n = 0.81056$ mol							
270.709	12.062	440060.	108.51	108.16	301.377	11.050	1032700.	117.33	118.85	285.681	11.591	683430.	112.62	112.86
273.039	11.991	472850.	108.98	108.70	303.770	10.962	1095600.	117.51	119.30	288.051	11.512	729540.	112.70	113.08
275.379	11.919	507580.	109.50	109.29	306.161	10.873	1161200.	118.70	120.81	290.431	11.433	778110.	114.03	114.57
277.720	11.846	544190.	110.58	110.44	308.571	10.781	1230100.	119.59	122.04	292.813	11.352	829060.	115.06	115.77
280.068	11.772	582830.	110.96	110.92	310.980	10.687	1302100.	120.80	123.64	295.206	11.269	882670.	115.09	116.00
282.414	11.697	623440.	112.12	112.19	313.405	10.591	1377500.	121.42	124.69	297.595	11.186	938700.	115.86	116.98
284.774	11.620	666370.	112.86	113.05	315.831	10.492	1456100.	121.24	124.99	299.996	11.100	997580.	116.90	118.27
287.131	11.543	711380.	112.76	113.09	271.488	12.038	450830.	109.58	109.25	302.399	11.013	1059200.	117.92	119.55
289.496	11.464	758750.	113.70	114.17	273.846	11.966	484620.	109.35	109.09	304.811	10.923	1123800.	118.34	120.27
291.863	11.384	808450.	114.31	114.95	276.202	11.893	520230.	109.91	109.72	307.226	10.832	1191300.	119.06	121.32
294.237	11.303	860670.	114.47	115.29	278.568	11.819	557920.	110.78	110.68	309.646	10.739	1261900.	119.32	121.95
296.613	11.220	915360.	115.52	116.56	280.932	11.744	597550.	111.66	111.66	312.069	10.644	1335600.	120.43	123.46
298.993	11.136	972660.	116.54	117.80	283.301	11.668	639330.	112.67	112.78	314.507	10.546	1412800.	120.65	124.14

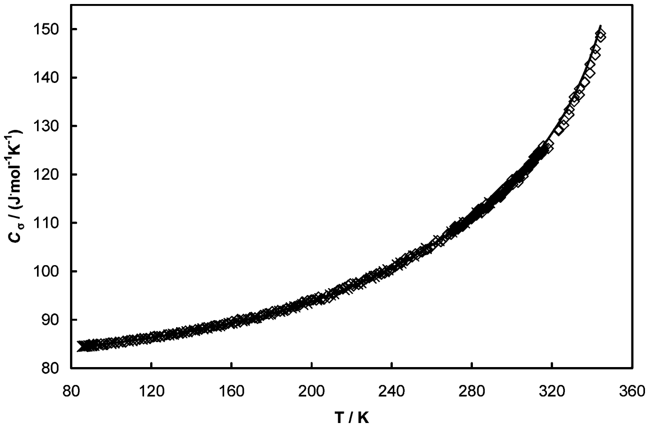

Figure 4. Heat capacity of saturated liquid propane (C_σ) from (88 to 345) K where: ◇, present results for $n = 0.69081$ mol; ◆, present results for $n = 0.81056$ mol; ×, Goodwin[8] for $n = 0.8288$ and 0.9213 mol; and the solid line is calculated with the equation of state of Lemmon et al.[3]

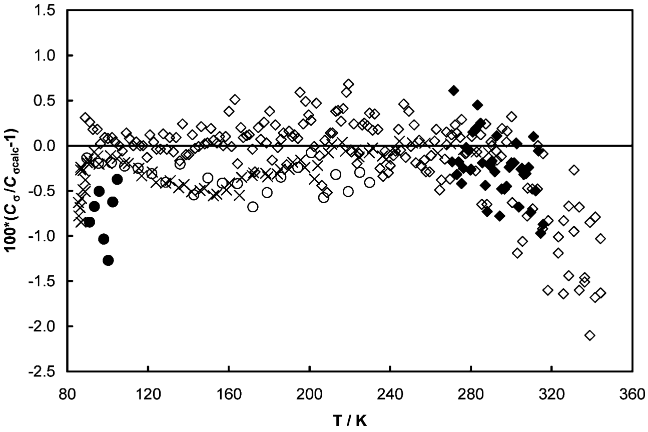

Figure 5. Relative deviations between data for heat capacity of saturated liquid propane (C_σ) and values calculated with the equation of state of Lemmon et al.[3] at temperatures from (88 to 345) K, where: ◇, present results for $n = 0.69081$ mol; ◆, present results for $n = 0.81056$ mol; and ×, Goodwin[8] for $n = 0.8288$ and 0.9213 mol. Low-temperature C_P (less than 1 bar) deviations that are nearly equal to C_σ are also shown, where: ●, Cutler and Morrison;[21] and ○, Kemp and Egan.[16]

measurements for this analysis. Values for $U^{(2)}$ at two or more densities are needed to calculate the change of the bulk internal energy with respect to the bulk molar volume at constant temperature. Since the calorimetric measurements provide the change of internal energy from one density to another, we need additional information at a reference temperature to determine the change of internal energy between two densities. This reference temperature is selected near the normal boiling point, where accurate, direct measurements of the vapor pressure are available.

The value of $(\partial U^{(2)}/\partial V^{(2)})_T$ at the reference temperature can be calculated with eq 6 and vapor pressure data around the reference temperature. Then, the change of internal energy from density 1 to density 2 at that reference temperature can be determined from

$$U_2^{(2)} - U_1^{(2)} = (V_2^{(2)} - V_1^{(2)})\left(\frac{\partial U^{(2)}}{\partial V^{(2)}}\right)_T \tag{8}$$

In the present analysis, we set the internal energy of one of these states $U_1^{(2)}$ to an arbitrary value of zero at the reference temperature. Then internal energy increments are calculated at each temperature and density based on differences in U from this reference state. Since the present two-phase measurements are at relatively high densities, it is appropriate to select the vapor phase at saturation for the low density state 1 in eq 8. At each temperature considered, $U_1^{(2)}$ and $V_1^{(2)}$ are calculated with the equation of state of Lemmon et al.[3] for the saturated vapor phase of propane, with the constraint that $U_1^{(2)} = 0$ at the reference temperature.

A temperature of 240 K was selected as the reference temperature in the present analysis since the normal boiling point of propane is near 231 K, where vapor pressures can be directly measured with low uncertainty, and the properties of the vapor phase approach those of the ideal gas. The accurate vapor pressure data of Glos et al.[22] in the vicinity of 240 K form the basis for analysis of the derived vapor-pressure data from the present calorimetric measurements. Bücker and Wagner[26] demonstrate that the vapor pressure of propane is well represented by an equation of the form

$$\ln\left(\frac{P_\sigma}{P_c}\right) = \frac{1}{1-\tau}(C_1\tau + C_2\tau^{1.5} + C_3\tau^{2.5} + C_4\tau^5 + C_5\tau^{7.5}) \tag{9}$$

where $\tau = (1 - T/T_c)$; $T_c = 369.825$ K; $P_c = 4247.66$ kPa: and C_i are empirical coefficients. These authors were able to accurately represent the best available vapor pressure data for propane from the triple point to the critical point with eq 9, including the wide-range data of Glos et al.[22] Equation 9 is selected as the functional form to represent vapor pressures during the present analysis at temperatures from the triple point to 240 K. The derivative of vapor pressure with respect to temperature, as represented by eq 9, is also required for evaluation of eq 6

$$\frac{dP_\sigma}{dT} = -\frac{P_\sigma}{T}\left[\ln\left(\frac{P_\sigma}{P_c}\right) + C_1 + 1.5C_2\tau^{.5} + 2.5C_3\tau^{1.5} + 5C_4\tau^4 + 7.5C_5\tau^{6.5}\right] \tag{10}$$

Equation 7 was evaluated from two-phase calorimetric data along an isochore at temperatures from (88 to 250) K with the calorimeter filled with $n = 0.69081$ mol of propane. The change in internal energy along this isochore was determined from a quadratic fit in temperature to these calorimetric data over the temperature range from (88 to 300) K. The energy needed to increase the temperature of the sample by ΔT is given by

$$\frac{Q}{n\Delta T} = a_0 + a_1T + a_2T^2 + a_3T^3 \tag{11}$$

where Q is the energy pulse (J); n is the amount of substance (mol); and T is the sample temperature (K). The coefficients are $a_0 = 8.28315731\cdot10^1$, $a_1 = 2.09141766\cdot10^{-2}$, $a_2 = -1.17351339\cdot10^{-4}$, and $a_3 = 1.51729678\cdot10^{-6}$. The change of internal energy along this isochore is given by the expression

$$\Delta U = \int_{T_1}^{T_2} \frac{Q}{n\Delta T}\mathrm{d}T \tag{12}$$

Although the bomb volume varies with temperature and pressure, we may approximate the density as a function of temperature only due to the low vapor pressure over this temperature range. The density of this pseudoisochore at temperatures from (88 to 300) K was fit to the equation

$$\rho = b_0 + b_1T + b_2T^2 \tag{13}$$

where ρ is in mol·L^{-1} and the coefficients are $b_0 = 3.95842164\cdot10^2$, $b_1 = -1.08799944\cdot10^{-2}$, and $b_2 = -1.63589568\cdot10^{-5}$.

The internal energy of the saturated vapor was calculated from the equation of state of Lemmon et al.[3] for propane. Previous analysis[25] has shown that the results are insensitive to the choice of a gas-phase equation of state as long as it reproduces the correct behavior of the second virial coefficients. A value of $(\partial U^{(2)}/\partial V^{(2)})_T$ was calculated at the reference temperature of 240 K with the ancillary equation for the vapor pressure of propane of Lemmon et al.[3] Application of the method described above to calculate vapor pressures from the measured internal energy increments resulted in optimum coefficients for the vapor pressure expression of eq 9. These coefficients are $C_1 = -6.73240923$, $C_2 = 1.43841958$, $C_3 = -1.37355509$, $C_4 = -2.66389002$, and $C_5 = 7.44870619 \cdot 10^{-1}$. It must be emphasized that these coefficients are optimized for the temperature range from the triple point to 240 K, and eq 9 should not be used with these coefficients at temperatures above 240 K. At temperatures above 240 K, the ancillary expression of Lemmon et al.[3] is more accurate. Table 3 provides the vapor pressures calculated from internal energy increments, along with values calculated with the equation of state of Lemmon et al.[3] for propane. Figure 6 shows deviations between the present vapor pressures derived from C_σ, along with data from the literature, relative to the equation of state of Lemmon et al.[3] at temperatures from the triple point to 240 K. It is noteworthy that the present values are in excellent agreement with the direct measurements of Glos et al.[22] at temperatures up to 240 K. Direct measurement of vapor pressure becomes increasingly difficult and subject to errors due to the presence of volatile impurities at very low reduced temperatures. Figure 7 focuses on the vapor-pressure deviations at the lowest temperatures, from the triple point to 130 K. The present values are in better agreement with the data of Tickner and Lossing[23] (orfice-mass selective detector) and Carruth and Kobayashi[24] (gas saturation) than the direct pressure measurements of Glos et al.[22] over this temperature region. It appears that these two indirect techniques were less sensitive to impurities at the lowest pressures. However, agreement is excellent (less than 0.4 Pa) and within claimed uncertainties for all measurements at temperatures below 130 K. It is also apparent in Figure 7 that there were no data available at temperatures below 94 K prior to the present work. On the basis of the present vapor pressure results, the triple-point pressure of propane is 0.000176 Pa at the triple-point temperature of 85.525 K reported above. This agrees well with the value of 0.0002 Pa reported by Glos et al.[22]

Table 3. Vapor Pressure P_σ Values Derived from the Present Saturated Liquid Heat Capacity C_σ Data for Propane at Temperatures from (85.525 to 241) K[a]

T	P_σ	$P_{\sigma,\mathrm{calc}}$	ΔP_σ	
K	Pa	Pa	Pa	$100 \cdot \Delta P_\sigma / P_{\sigma,\mathrm{calc}}$
85.525	0.000176	0.000172	0.000004	2.2981
88.000	0.000465	0.000458	0.000007	1.4864
91.000	0.001405	0.001391	0.000014	1.0282
94.000	0.003935	0.003910	0.000025	0.6404
97.000	0.010297	0.010258	0.000039	0.3846
100.000	0.025320	0.025272	0.000048	0.1900
103.000	0.058842	0.058806	0.000036	0.0610
106.000	0.129859	0.129889	−0.000030	−0.0228
109.000	0.273346	0.273539	−0.000193	−0.0705
112.000	0.550918	0.551429	−0.000511	−0.0927
115.000	1.066854	1.067879	−0.001025	−0.0960
118.000	1.991225	1.992951	−0.001726	−0.0866
121.000	3.592144	3.594624	−0.002480	−0.0690
124.000	6.279251	6.282179	−0.002928	−0.0466
127.000	10.660580	10.662946	−0.002366	−0.0222
130.000	17.614853	17.614446	0.000407	0.0023
133.000	28.380953	28.373715	0.007238	0.0255
136.000	44.665932	44.645194	0.020738	0.0465
139.000	68.772387	68.728015	0.044372	0.0646
142.000	103.745372	103.662912	0.082460	0.0795
145.000	153.538338	153.398244	0.140094	0.0913
148.000	223.196856	222.973909	0.222947	0.1000
151.000	319.058176	318.721192	0.336984	0.1057
154.000	448.964014	448.475950	0.488064	0.1088
157.000	622.483442	621.801945	0.681497	0.1096
160.000	851.142276	850.220706	0.921570	0.1084
163.000	1148.655087	1147.444012	1.211076	0.1055
166.000	1531.155828	1529.604885	1.550943	0.1014
169.000	2017.423024	2015.483068	1.939956	0.0963
172.000	2629.095668	2626.721008	2.374660	0.0904
175.000	3390.876184	3388.026743	2.849441	0.0841
178.000	4330.717212	4327.360391	3.356821	0.0776
181.000	5479.989431	5476.101472	3.887959	0.0710
184.000	6873.628130	6869.194792	4.433338	0.0645
187.000	8550.256795	8545.273208	4.983587	0.0583
190.000	10552.286545	10546.756149	5.530396	0.0524
193.000	12925.990808	12919.923363	6.067445	0.0470
196.000	15721.555137	15714.963865	6.591272	0.0419
199.000	18993.102579	18986.000571	7.102008	0.0374
202.000	22798.695440	22791.091527	7.603913	0.0334
205.000	27200.314656	27192.209002	8.105654	0.0298
208.000	32263.818334	32255.198032	8.620302	0.0267
211.000	38058.881236	38049.716207	9.165029	0.0241
214.000	44658.917224	44649.156686	9.760538	0.0219
217.000	52140.986763	52130.556529	10.430234	0.0200
220.000	60585.691712	60574.492474	11.199238	0.0185
223.000	70077.059616	70064.966335	12.093281	0.0173
226.000	80702.419735	80689.282143	13.137592	0.0163
229.000	92552.272962	92537.917117	14.355845	0.0155
232.000	105720.157749	105704.388470	15.769279	0.0149
235.000	120302.513998	120285.117940	17.396058	0.0145
238.000	136398.546829	136379.295900	19.250929	0.0141
241.000	154110.091948	154088.746670	21.345278	0.0139

[a] These derived values are compared with the values calculated with the equation of state of Lemmon et al.[3]

Assessment of Uncertainties. Uncertainty in C_V is limited by the uncertainty of the temperature rise measurement and the change-of-volume work adjustment. In the following discussion, the definition for the expanded uncertainty, which is two times the standard uncertainty, corresponds to a coverage factor $k = 2$ and thus a two-standard-deviation estimate. The triple-point measurements of argon and propane reported in this work indicate that the calibration of the platinum resistance thermometer presently has an uncertainty of 0.003 K near the ITS-90 fixed point for argon at its triple point (83.8058 K). Different sources of uncertainty, including calibration of the platinum resistance thermometer, radiation to or from the thermometer head, and drift in the resistance at temperature-scale fixed points, contribute to an expanded uncertainty of 0.01 K at 100 K to 0.03 K at 345 K for the absolute temperature measurement during C_V measurements. The uncertainty of the temperature rise also depends on reproducibility of temperature measurements. The temperatures assigned to the beginning (T_1) and to the end (T_2) of a heating interval are determined by extrapolation of a linear temperature drift (approximately $-1 \cdot 10^{-3}$ K·min^{-1} to $0.5 \cdot 10^{-3}$ K·min^{-1}) to the midpoint time of the interval. This procedure leads to an uncertainty of (0.01 to 0.04) K for the extrapolated temperatures T_1 and T_2, depending on the standard deviation of the linear fit. In all cases, values from (0.002 to 0.006) K were obtained for the uncertainty of the temperature rise, $\Delta T = T_2 - T_1$. For a typical experimental value of $\Delta T = 4$ K, this corresponds to a relative uncertainty of between 0.05 % and 0.15 %.

The uncertainty of the change-of-volume work adjustment has a larger influence on the single phase values, since two-phase experiments are performed over a smaller pressure interval. The ratio of change-of-volume work to total applied

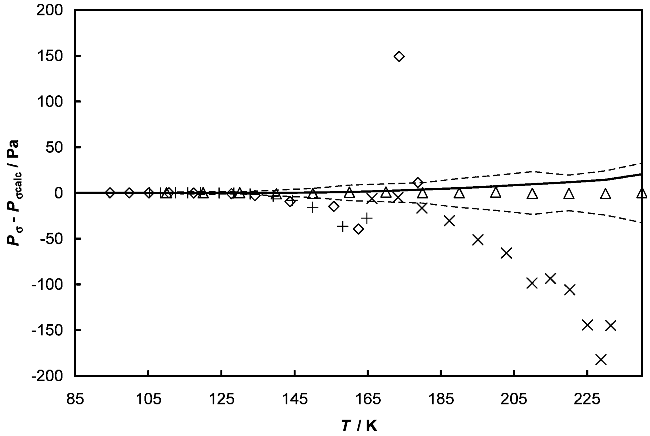

Figure 6. Deviations between vapor-pressure (P_σ) values and the vapor-pressure expression of Lemmon et al.[3] for propane (P_σ) at temperatures from (85.525 to 240) K. The solid line represents P_σ values derived from the present saturated-liquid heat capacity C_σ data. Literature data for P_σ are shown as: Δ, Glos et al.;[22] +, Tickner and Lossing;[23] ◇, Carruth and Kobayashi;[24] and ×, Kemp and Egan.[16] The dashed lines show the uncertainty bounds for the data of Glos et al.[22]

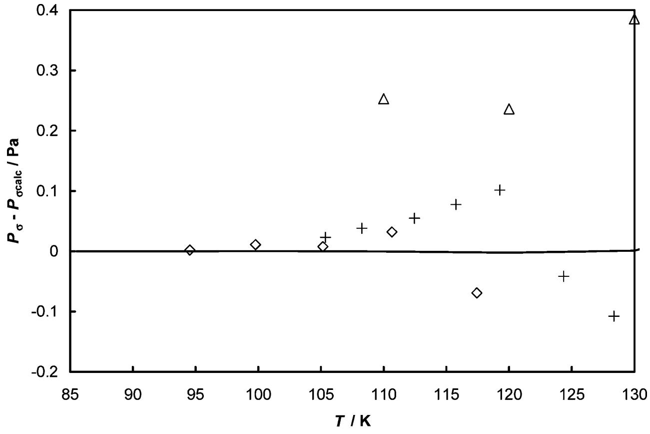

Figure 7. Deviations between vapor pressure (P_σ) values and the vapor pressure expression of Lemmon et al.[3] for propane (P_σ) at temperatures from (85.525 to 130) K. The solid line represents P_σ values derived from the present saturated liquid heat capacity C_σ data. Literature data for P_σ are shown as: Δ, Glos et al.;[22] +, Tickner and Lossing;[23] and ◇, Carruth and Kobayashi.[24]

heat may be as large as 0.11 for the highest-density isochore down to 0.005 at the lowest densities. Estimated uncertainties of 2.3 % to 3.0 % in the change-of-volume work adjustment are due to both the deviation of the calculated pressure derivatives and the uncertainty of the volume change. This leads to a relative uncertainty of 0.2 % in C_V for the lowest density isochore up to 0.3 % for the highest density.

The energy applied to the calorimeter is the integral of the product of voltage and current from the initial to the final heating time. Voltage and current are measured 20 times during a heating interval. The measurements of the electrical quantities have a relative uncertainty of 0.01 %. However, we must account for the effect of radiation heat losses or gains, which occur when a time-dependent lag of the controller leads to a small temperature difference of about 20 mK between the bomb and the radiation shield at the beginning and end of a heating period. Since heat transfer by radiation is proportional to $(T_1^4 - T_2^4) \approx 4 \cdot T^3 \cdot \Delta T$, radiation losses should increase substantially with the bomb temperature. Therefore, the relative uncertainty in the applied heat is estimated to be 0.02 % for lower temperatures and up to 0.10 % for the highest temperatures. This leads to a relative uncertainty in C_V between 0.04 % and 0.2 %.

The energy applied to the empty calorimeter has been measured in repeated experiments and fitted to a function of temperature;[3] its relative uncertainty is less than 0.02 %. Its influence on the uncertainty of the heat capacity is reduced because the ratio of the heat applied to the empty calorimeter to the total heat varies only from 0.35 to 0.70 for the single-phase runs and from 0.61 to 0.62 for the two-phase runs. The mass of each sample was determined with a relative uncertainty of 0.01 % by differential weighing before and after trapping the sample. The density calculated from this mass and the bomb volume has a relative uncertainty of 0.02 %. For pressures, the uncertainty of the transducer of 7 kPa is added to the cross term for the pressure derivative in the change-of-volume work adjustment. However, neither the uncertainty of P nor ρ contributes appreciably to the combined uncertainty for molar heat capacity. When the various sources of experimental uncertainty are combined using a root-sum-of-squares formula, the expanded relative uncertainty is estimated to 0.7 % for C_V, 0.5 % for $C_\text{V}^{(2)}$, and 0.7 % for C_σ.

Conclusions

Calorimetric measurements were conducted on liquid propane in equilibrium with its vapor and on compressed liquid propane along isochores. The heat capacity C_V was measured as a function of temperature and density at a total of 231 single-phase and 223 two-phase states for propane. Molar heat capacity results are reported for two-phase ($C_\text{V}^{(2)}$), saturated liquid (C_σ), and single-phase (C_V) isochores. Temperatures ranged from the triple point of propane near 85 K to the upper temperature limit of the calorimeter at 345 K, while pressures ranged from (0 to 35) MPa. Vapor-pressure data are reported that are based on measurements of $C_\text{V}^{(2)}$ along a two-phase isochore. Measurements were also made to determine the triple-point temperature of (85.525 ± 0.005) K and heat of fusion of (3508 ± 20) $\text{J} \cdot \text{mol}^{-1}$ for propane. The principal sources of uncertainty are the temperature-rise measurement and the change-of-volume work adjustment. The expanded relative uncertainty (i.e., a coverage factor $k = 2$ and thus a two-standard-deviation estimate) for values of $C_\text{V}^{(2)}$ is estimated to be 0.5 %; for both C_σ and C_V, it is 0.7 %. These measurements for the heat capacity of propane agree well with previous heat capacity measurements and the Helmholtz energy model of Lemmon et al.[3]

Acknowledgment

We thank Eric Lemmon and Mark McLinden for generous technical assistance and helpful discussions during this study and Tom Bruno for analysis of the purity of the propane sample.

Supporting Information Available:

Measurement of the triple-point temperature of argon and calibration of the calorimeter volume as a function of temperature and pressure based on the density of propane[3] are reported. This material is available free of charge via the Internet at http://pubs.acs.org.

Literature Cited

(1) McLinden, M. O. Thermodynamic Properties of Propane. I. Density. *J. Chem. Eng. Data* **2009**, in press.

(2) Meier, K. Thermodynamic Properties of Propane. IV. Sound Speed. *J. Chem. Eng. Data* **2009**, to be submitted.

(3) Lemmon, E. W.; McLinden, M. O.; Wagner, W. Thermodynamic Properties of Propane. III. A Reference Equation of State for Temperatures from the Melting Line to 650 K and Pressures up to 1000 MPa. *J. Chem. Eng. Data* **2009**, in press.

(4) Goodwin, R. D. Apparatus for determination of pressure-density-temperature relations and specific heats of hydrogen to 350 atm at temperatures above 14 degrees K. *J. Res. Natl. Bur. Stand.* **1961**, *65C*, 231–243.

(5) Younglove, B. A. The specific heats, C(sigma), and C(v), of compressed and liquefied methane. *J. Res. Natl. Bur. Stand.* **1974**, *78A*, 401–410.

(6) Roder, H. M. Measurements of the specific heats, C(sigma), and C(v), of dense gaseous and liquid ethane. *J. Res. Natl. Bur. Stand.* **1976**, *80A*, 739–759.

(7) Mayrath, J. E.; Magee, J. W. Measurements of molar heat capacity at constant volume: C(V,m){xCH(4) + (1-x}C(2)H(6), $T = 100$ to 320 K, $p < 35$ MPa}. *J. Chem. Thermodyn.* **1989**, *21*, 499–513.

(8) Goodwin, R. D. Specific heats of saturated and compressed liquid propane. *J. Res. Natl. Bur. Stand. (U. S.)* **1978**, *83*, 449–458.

(9) Magee, J. W. Molar heat capacity (C_V) for saturated and compressed liquid and vapor nitrogen from 65 to 300 K at pressures to 30 MPa. *J. Res. Natl. Inst. Stand. Technol.* **1991**, *96*, 725–740.

(10) Magee, J. W.; Luddecke, T. O. D. Molar heat capacity at constant volume of n-butane at temperatures from 140 to 342 K and at pressures to 33 MPa. *Int. J. Thermophys.* **1998**, *19*, 129–144.

(11) Goodwin, R. D.; Weber, L. A. Specific heats of oxygen at coexistence. *J. Res. Natl. Bur. Stand.* **1969**, *73A*, 1–13.

(12) Wieser, M. E. Atomic Weights of the Elements 2005 (IUPAC Technical Report). *Pure Appl. Chem.* **2006**, *78*, 2051–2066.

(13) Pavese, F.; Besley, L. M. Triple-point temperature of propane: measurements on two solid-to-liquid transitions and one solid-to-solid transition. *J. Chem. Thermodyn.* **1981**, *13*, 1095–1104.

(14) Preston-Thomas, H. The international temperature scale of 1990 (ITS-90). *Metrologia* **1990**, *27*, 3–10.

(15) Hicks-Bruun, M. M.; Bruun, J. H. The freezing point and boiling point of propane. *J. Am. Chem. Soc.* **1936**, *58*, 810–2.

(16) Kemp, J. D.; Egan, C. J. Hindered rotation of the methyl groups in propane. The heat capacity, vapor pressure, heats of fusion and vaporization of propane. Entropy and density of the gas. *J. Am. Chem. Soc.* **1938**, *60*, 1521–1525.

(17) Bedford, R. E.; Bonnier, G.; Maas, H.; Pavese, F. Recommended values of temperature on the international temperature scale of 1990 for a selected set of secondary reference points. *Metrologia* **1996**, *33*, 133–154.

(18) Anisimov, M. A.; Beketov, V. G.; Voronov, V. P.; Nagaev, V. B.; Smirnov, V. A. Experimental study of the isochoric heat capacity of propane in the one- and two- phase regions. *Thermophys. Prop. Subst.* **1982**, *16*, 48–59.

(19) Abdulagatov, I. M.; Levina, L. N.; Zakaryaev, Z. R.; Mamchenkova, O. N. Thermodynamic properties of propane in the critical region. *J. Chem. Thermodyn.* **1995**, *27*, 1385–1406.

(20) Rowlinson, J. S. *Liquids and Liquid Mixtures*; Butterworths: London, 1969.

(21) Cutler, A. J. B.; Morrison, J. A. Excess thermodynamic functions for liquid mixtures of methane+propane. *Trans. Faraday Soc.* **1965**, *61*, 429–442.

(22) Glos, S.; Kleinrahm, R.; Wagner, W. Measurement of the ($p,\rho,$T) relation of propane, propylene, n-butane, and isobutane in the temperature range from (95 to 340) K at pressures up to 12 MPa using an accurate two-sinker densimeter. *J. Chem. Thermodyn.* **2004**, *36*, 1037–1059.

(23) Tickner, A. W.; Lossing, F. P. The measurement of low vapor pressures by means of a mass spectrometer. *J. Phys. Colloid Chem.* **1951**, *55*, 733–40.

(24) Carruth, G. F.; Kobayashi, R. Vapor pressure of normal paraffins ethane through n-decane from their triple points to about 10 mm Hg. *J. Chem. Eng. Data* **1973**, *18*, 115–26.

(25) Duarte-Garza, H. A.; Magee, J. W. Subatmospheric vapor pressures evaluated from internal-energy measurements. *Int. J. Thermophys.* **1997**, *18*, 173–193.

(26) Bücker, D.; Wagner, W. Reference equations of state for the thermodynamic properties of fluid phase n-butane and isobutane. *J. Phys. Chem. Ref. Data* **2006**, *35*, 929–1019.

Received for review January 30, 2009. Accepted April 27, 2009.

JE900137R